

Copyright
by
Benjamin Grady Marshall
2021

**The Thesis Committee for Benjamin Grady Marshall
Certifies that this is the approved version of the following Thesis:**

**Artificial Trichome Copper Mesh for Dehumidification Purposes in
Architecture**

**APPROVED BY
SUPERVISING COMMITTEE:**

Juliana Felkner, Supervisor

Michelle Addington, Co-Supervisor

Zoltan Nagy

**Artificial Trichome Copper Mesh for Dehumidification Purposes in
Architecture**

by

Benjamin Grady Marshall

Thesis

Presented to the Faculty of the Graduate School of

The University of Texas at Austin

in Partial Fulfillment

of the Requirements

for the Degree of

Master of Science in Sustainable Design

The University of Texas at Austin

May 2021

Dedication

I would like to dedicate this thesis to my amazing wife Victoria. You helped put me through this degree and you have encouraged me to chase this dream.

Acknowledgements

I would like to acknowledge many people who have helped me through the degree and encouraged me in my future endeavors.

Professor Juliana Felkner, thank you for taking me under your wing and advising me through this thesis. Thank you also for encouraging me to continue my studies in a PhD here at the University of Texas at Austin.

Professor Atila Novoselac, I am glad I went to talk to you my first day on campus. Thank you for your mentorship and letting me use the Pickle Research facilities for this thesis. I look forward to studying for my PhD under your guidance.

Professor Matt Fajkus, thank you for encouraging me to go with the MSSD program even when I was kicking and screaming not to.

Professor Jassen Callender, thank you for all of the calls, emails, and chats about graduate school. I really appreciate your mentorship.

Professor Emily McGlohn thank you for giving me a chance as an undergraduate researcher and guest lecturer all those years ago. I never would have thought I would end up here, but I probably would not have if not for you.

Luke, I would never have tried this if you and I hadn't had all those conversations about air plants and dehumidification.

Abstract

Artificial Trichome Copper Mesh for Dehumidification Purposes in Architecture

Benjamin Grady Marshall, MSSD

The University of Texas at Austin, 2021

Supervisors: Juliana Felkner, Michelle Addington

This thesis studied the properties of switchable wettability copper mesh, which has been developed for separating oil and water mixtures for its ability to dehumidify air. It was theorized that the dendritic structure of the copper 1 and copper 2 oxides grown on the mesh could act like artificial trichomes, bump like structures found on some plants, which would allow the mesh to not only absorb water vapor but also drain liquid water. After constructing fourteen of the mesh samples and the multi pass testing apparatus, tests were conducted at various air speeds. It was determined that the mesh was passively dehumidifying the air at 0.017 grams per hour for the low air speed of 0.002 meters per second. However, with higher air speeds the test apparatus leaked too much for the dehumidification properties of the mesh to be recorded. It was also noted that the different deposition times for copper oxide when constructing the mesh did influence the rate of dehumidification that the mesh was able to achieve. The mesh was able to dehumidify as hypothesized but it was not able to form liquid water which could be drained away. This is

hypothesized to happen because the trichome nature of the mesh works via water surface tension which is not present in vapor water.

Table of Contents

List of Tables	ix
List of Figures	x
List of Illustrations	xi
Artificial Trichome Copper Mesh for Dehumidification.....	1
1: Research Question	1
2: Previous Research.....	1
3: Methodology	4
4: Results.....	14
Apparatus Leakage.....	14
Fan Speed.....	17
Mesh Size.....	19
Mesh Construction	21
Electrical Input.....	23
Passive Water Absorption.....	25
5: Discussion and Conclusion	26
Fan Speed.....	27
Mesh size and Construction	27
Electrical input	27
Passive Water Absorption.....	28
Apparatus Sizing.....	30
Conclusion	30
References.....	32

List of Tables

Table 1:	Titration Calculations.....	5
Table 2:	Mesh construction times.	7
Table 3:	Loop sizing.....	10
Table 4:	Reynolds number calculations.	11
Table 5:	Fan pressure calculations.	12
Table 6:	LI-COR Flowrate.	13
Table 7:	Pressure drop across membranes.	13
Table 8:	Mesh Water Absorption calculations.....	28

List of Figures

Figure 1 & 2:	Mesh sample in electrolyte solution and mesh sample being dried.....	6
Figure 3:	Mesh samples organized.....	8
Figure 4 & 5:	Blast gate valve and 3d printed blast gate plate.....	8
Figure 6:	High Speed Fan Leak Test.....	16
Figure 7:	High Speed Fan Sealed Test.....	17
Figure 8:	High Fan Air Change Rate.....	18
Figure 9:	Low Speed Air Change Rate.....	18
Figure 10:	No Fan Test Air Change Rate.....	19
Figure 11:	H2O Mesh A.....	20
Figure 12:	H2O Mesh B.....	20
Figure 13:	A Meshes Comparison.....	21
Figure 14:	B Meshes Comparison.....	22
Figure 15:	Baseline vs Coated Meshes Comparison.....	23
Figure 16:	B1B No Fan Electrified Air Change Rate.....	24
Figure 17:	B7B No Fan Electrified.....	24
Figure 18:	B7B No Fan CO2 Concentration.....	25
Figure 19:	B7B No Fan Water Concentration.....	26

List of Illustrations

Illustration 1:	PVC test loop diagram.	9
Illustration 2:	"Reynolds Number & Pipe Flow" by Smith et al 2002, used under Creative Commons BY-NC-SA / Cropped from original handout.....	11
Illustration 3:	Dehumidification by mesh illustration.....	29

Artificial Trichome Copper Mesh for Dehumidification

1: Research Question

Is there a way to dehumidify air electrochemically or mechanically like biological systems (lotus leaf, air plants) rather than using psychometrics, the properties of water vapor at different temperatures in air, or desiccants, which require drying and eventual replacement?

2: Previous Research

Biomimicry refers to studying and using solutions found in nature to solve problems at human scale (Benyus 1997). One such solution can be found on the lotus leaf (Ensikat et al. 2011) with its extraordinary ability to shed water and keep its leaves clean. This happens due to specialized cells called Trichomes (Cheng et al. 2005). These cells are shaped like little bumps that are grouped close together on the leaf's surface. When water droplets fall on the leaf, the droplets only touch the trichomes which do not have a large surface area. Because of the water's surface tension and the small area of the trichomes, the water droplet stays spherical and the angle at which it touches the trichomes (the contact angle) stays large, at around 160 degrees (Ensikat et al. 2011). This phenomenon keeps the water droplets from sticking to the leaf and they are pulled off by gravity.

Trichomes are not only utilized to repel water but are also used by some plants in the Bromeliad family which includes air plants and Spanish mosses to pull water out of the air (Lusa et al. 2015). In this mode the trichomes secrete hydrophilic (water attracting) chemicals which pulls the water down in between the bump-like geometry of the trichomes to the surface of the leaf where it is absorbed by specialized cells. Because of the bump- or spike-like geometry of the trichomes, the surface area of the leaf is increased allowing the plant to trap water between the trichomes until it can be absorbed.

In the built environment, there are currently two main methods of dehumidification. These include cooling-based dehumidification and desiccant-based dehumidification (Harriman 2002). Cooling-based dehumidification uses the moisture capacity of air at different temperatures, psychometrics, to transform water from the vapor phase into the liquid phase. Once the air has been cooled down to a set temperature (usually around 55 degrees F or below) and a fraction of the water vapor has been condensed out of the air, this dehumidified air is used to condition buildings. In the liquid phase, the water is drained away from the building via the sanitary sewer, storm drainage, or is used for grey water in more sustainable constructions. This dehumidification method is energy intensive because the air is cooled below comfortable temperature before it is used (ASHRAE 2017) which is potentially wasteful.

Desiccant dehumidification is the second most common means of dehumidification currently used in buildings (Harriman 2002). Desiccants are materials which absorb water vapor out of the air. The attraction to water is usually a weak chemical bond which can be broken with the addition of heat. One of the most common desiccant dehumidification methods in the thermal comfort of buildings is a desiccant wheel or enthalpy wheel. This desiccant-covered wheel absorbs water vapor from incoming air. However, it must be regenerated, which is a process of removing water vapor from its weak bond by heating up the desiccant on the wheel. This dries out the wheel to allow the desiccant material to absorb water at a different location. This process is driven by the outgoing dry exhaust air from the building and supplemental heaters which use line energy. Desiccants must be dried by exposing them to dry (low relative humidity) air (Harriman, 2002). This dry air may be air from inside the building that has been dried by the desiccant or mechanical means or air that is heated up to provide more water vapor capacity before coming in contact with the saturated desiccant. The need for input energy to move water vapor from high relative humidity air to low relative humidity air works well when inside and outside temperatures are relatively different, but not when the temperatures are relatively similar. This means during shoulder seasons, when the temperature of the air may be within the

comfort zone (ASHRAE-55, 2017) but the humidity is too high, desiccants will not be as useful for providing thermal comfort (Harriman, 2002).

Thermal comfort, defined by the American Society of Heating Refrigeration and Air conditioning Engineers, is the conditions at which 80% of the occupants of a space would find acceptable (ASHRAE-55, 2017). The conditions of the space include:

1. Metabolic Rate
2. Clothing insulation
3. Air temperature
4. Radiant temperature
5. Air speed
6. Humidity

The humidity found acceptable by ASHRAE is any ratio of humidity below 0.012 (mass H₂O/mass of dry air). According to this definition of thermal comfort there is a range of temperatures for which someone may be comfortable if the humidity was not so high (humidity ratios roughly between 0.012-0.0245) (ASHRAE-55, 2017). To achieve thermal comfort, humidity need only be reduced in these situations.

Another element of the intersection of humidity and buildings to consider is the quality of the indoor air. Because moisture is an essential to the life of large and small organisms, having indoor air that is too humid can lead to health complications for occupants. A study performed in Sweden (Bornehag 2001) showed that dampness in buildings caused an increase in asthma, coughing and even headaches.

Moisture, in water vapor form, affects thermal comfort and the health of building occupants, and its removal is a major concern for engineers and architects. A possible solution to the water vapor problem may be found in a new material developed by researchers from the University of British Columbia (Kung et al 2018). This material is a mesh, woven strands, of pure copper that has been treated in an electrochemical process that grows copper-based crystals like the natural trichomes previously discussed. The advantageous part of this material for dehumidification is its ability to be both superhydrophobic, repelling water like a lotus leaf, and superhydrophilic, absorbing water

like a chemical desiccant. The researchers at the University of British Columbia (UBC) used this mesh to separate water from oil for use in industrial or oil spill clean-up applications, however they did not test the meshes ability to remove water from air.

3: Methodology

There were no samples of the mesh developed by Kung et al. (2018) available at The University of Texas at Austin with which to test. The methodology for testing this material was first to build it, then to test it. A mini Materials grant was procured from the Materials Lab at The University of Texas at Austin for most of the supplies needed to construct the mesh material. The process for electrodeposition of the mesh followed that of Kung et al. (2018). The only difference was due to the lack of laboratory equipment namely the Ag/AgCl reference electrode, but similar results were expected using the variable DC power supply (RoMech 30V DC Power Supply) procured through the grant. The meshes procured (.15mm and 2mm) were cleaned using acetone, isopropyl alcohol, and deionized water. Squares of the copper mesh (101.6x101.6mm) were hung by copper wire into an electrolyte solution of 0.1M copper Sulfate, 0.1M sodium sulfate, and 0.1M sulfuric acid. The solution was titrated using the following table.

Solid Components						
Titration Calculations	Formula	Desired Molar Concentration (mol/L)	Mols needed	Grams per Mol	Grams needed	Kg Needed
Copper Sulfate (blue crystals/pentahydrate)	CuSO ₄ ·5H ₂ O	0.1	0.16	249.685	39.9496	0.03995
Sodium Sulfate (anhydrous)	Na ₂ SO ₄	0.1	0.16	142.04	22.7264	0.02273
Sulfuric Acid	H ₂ SO ₄	0.1	0.16	98.079	15.69264	0.01569
Volume of Final Solution			1.6 Liters			
Liquid Components						
Density (g/cm ³ AKA g/mL)	mL needed	Concentration of current solution (mol/L)	Amount of Solution (L)	# of Moles available	L of solution needed	mL of solution needed
3.6	11.09711111					
2.664	8.530930931					
1.8302	8.574276035	1	0.5	0.5	0.16	160
Liters of dissolved chemicals	0.028202318					
Amount of pure Water needed (distilled)			1.571797682 Liters			

Table 1: Titration Calculations.

Using the DC power supply, 1.5V was passed through the solution for 100 seconds and then lowered to 0.2V for 20 seconds. Subsequent mesh samples were submerged for increased time in the solution while keeping to the same 10:2 ratio.

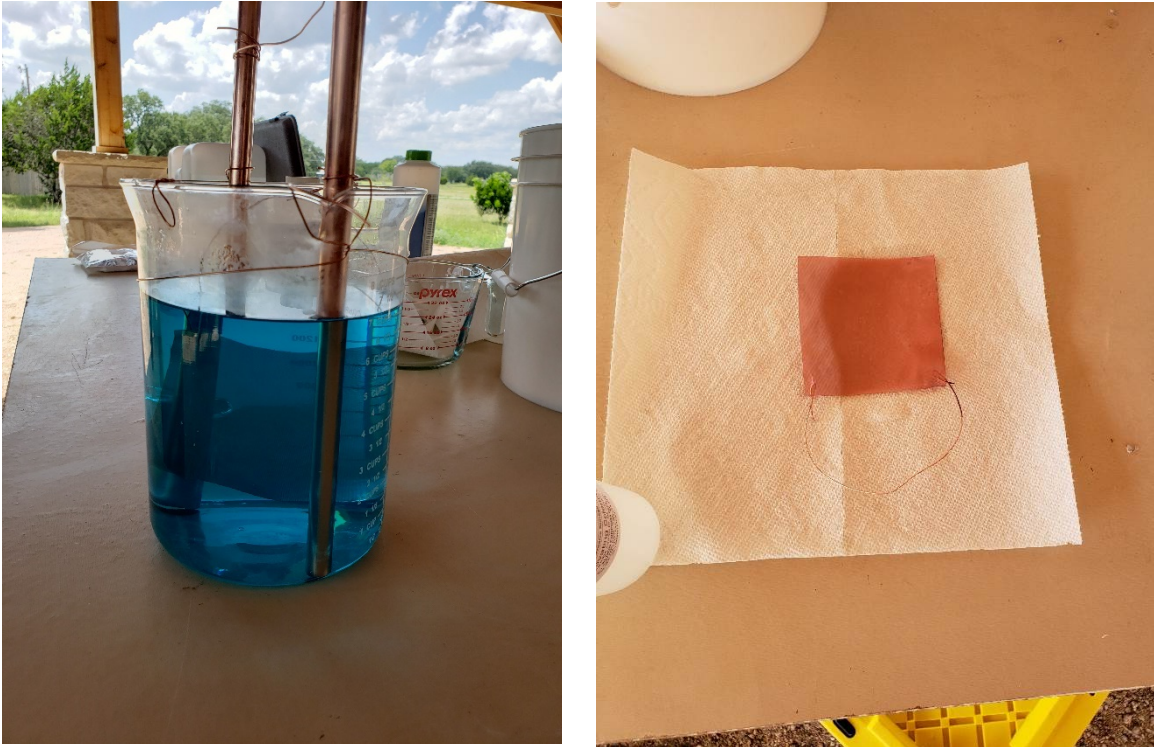


Figure 1 & 2: Mesh sample in electrolyte solution and mesh sample being dried.

The mesh sample studied by Kung et al. was 4mmx4mm and it was hypothesized that more time would be needed to electrolytically deposit the correct amount of copper oxide which was the reason for increasing the time of the mesh sample submersion. The power supply was then be turned off and the mesh removed for rinsing with deionized water and air drying for 1 hour. Below is a table of the mesh samples created for testing.

Sample	Mesh size	Voltage 1	Time 1	Amp current 1	Voltage 2	Time 2	Amp current 2
B1A	150/in	1.5 V	100 sec	2.12 Amps	.2 V	20 sec	.32 Amps
B1B	60/in	1.5 V	100 sec	1.65 Amps	.2 V	20 sec	.47 Amps
B2A	150/in	1.5 V	150 sec	1.44 Amps	.2 V	30 sec	??
B2B	60/in	1.5V	150 sec	1.37 Amps	.2 V	30 sec	.35 Amps
B3A	150/in	1.5 V	200 sec	1.5 Amps	.2 V	40 sec	.32 Amps
B3B	60/in	1.5 V	200 sec	1.53 amps	.2 V	40 sec	.35 Amps
B4A	150/in	1.5 V	250 sec	1.38 Amps	.2 V	50 secs	.21 Amps
B4B	60/in	1.5 V	250 sec	1.48 Amps	.2 V	50 secs	.21 Amps
B5A	150/in	1.5 V	300 sec	1.5 Amps	.2 V	60 secs	.32 Amps
B5B	60/in	1.5 V	300 sec	1.3 Amps	.2 V	60 secs	.21 Amps
B6A	150/in	1.5 V	350 sec	1.5 Amps	.2 V	70 secs	.16 Amps
B6B	60/in	1.5 V	350 sec	1.28 Amps	.2 V	70 secs	.26 Amps
B7A	150/in	1.5 V	400 sec	1.15 Amps	.2V	80 sec	.32 Amps
B7B	60/in	1.5 V	400 sec	1.29 Aps	.2V	80 Sec	.1 Amps

Table 2: Mesh construction times.

Pictured below are the fourteen samples with the wider pore mesh (60/in) above and the smaller pore mesh (150/in) below).

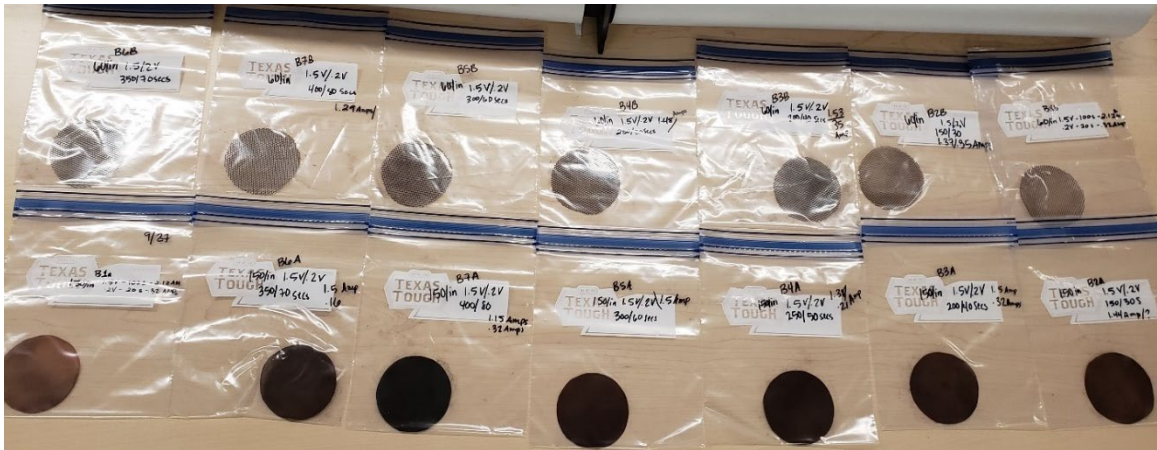


Figure 3: Mesh samples organized.

Upon drying the mesh was placed in the center of a 5-foot by 2-foot loop of 4" PVC pipe via a modified blast gate valve from a dust collection system. The blast gate was

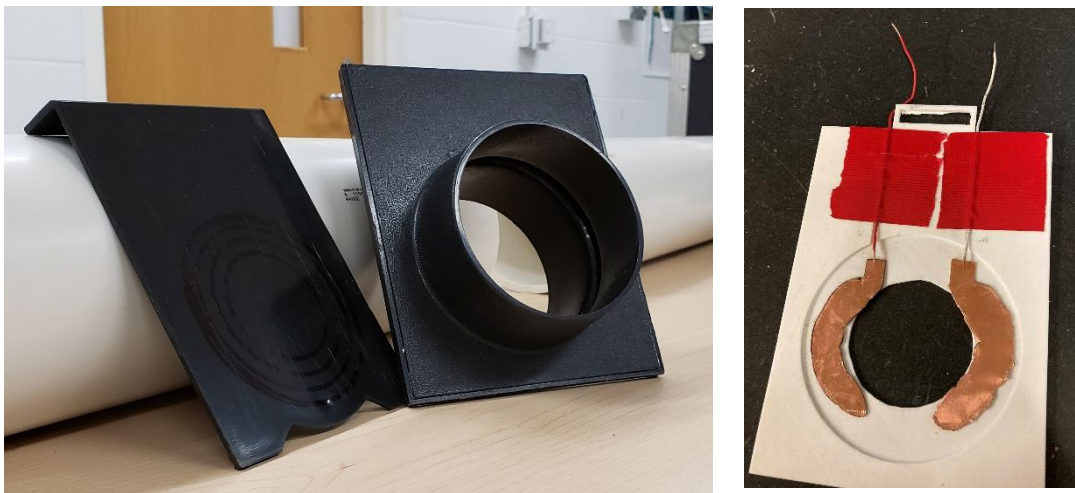


Figure 4 & 5: Blast gate valve and 3d printed blast gate plate.

implemented to facilitate easy switching of different samples without having to dismantle the testing apparatus. The blast gate plate (pictured on the left) was removed and a 3d printed blast gate plate with an aperture for air flow and wire routing channels was used. Since the samples were to be electrified a pair of copper plates were cut to frame the

opening so that electrical resistance would cause the charge to be evenly distributed across the screen.

An electric inline fan was placed into the PVC loop and three holes were drilled into the loop for addition of water vapor and test inputs and outputs. The tool used to measure the water vapor in the loop was the LI-COR 7000, which measures both CO₂ in ppm and H₂O in mmol/mol. The tool can measure down to a tenth of a millimole and will output readings to the hundredth of a millimole although for this test the accuracy was assumed to be in the +/- 0.1 mmol/mol range.

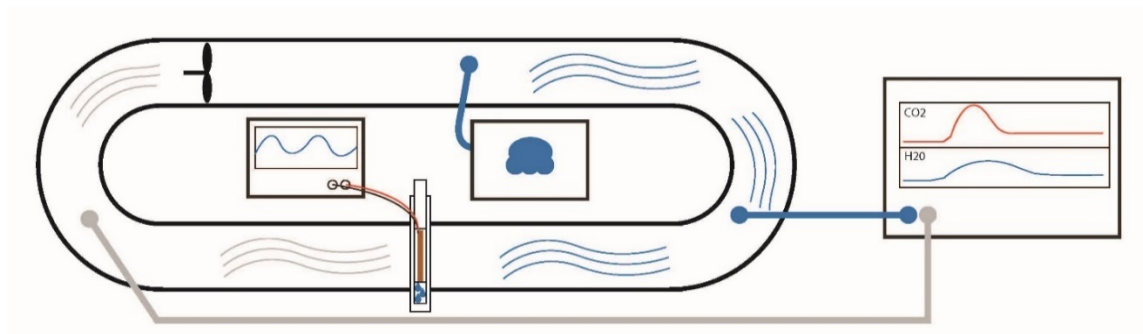


Illustration 1: PVC test loop diagram.

The PVC loop was sized so that slight changes in humidity would be around 0.1% but no larger or smaller.

	Licor 7000	mmol/mol	Allowable difference g/kg
			0.000622109
Water Vapor	18.02	g/mole	0.01802
Air	28.966	g/mole	28.966
% Error	1%	0.062210868	g water vapor needed in order for allowable difference to be 1 % error
		0.004921948	kg of air
		0.004203018	m3 of air
4" pipe	hydraulic diameter [4 inch]	0.1016	meters
4" pipe	area	0.00810321	meters cubic
4" pipe	length	0.607407276	meters
	Volume needed	0.148428201	ft3 of air

Table 3: Loop sizing.

To determine the air velocity in the system for the adjustable fan, pressure measurements were taken with the fan at its different settings using the inlet and outlet holes drilled on the far sides of the loop. The goal was for the fan to supply laminar air flow, turbulent air flow, and air flow that was low enough to simulate natural ventilation. This was done using equations for Reynolds number and pipe flow (Smith et al 2002).

Reynolds Number & Pipe Flow

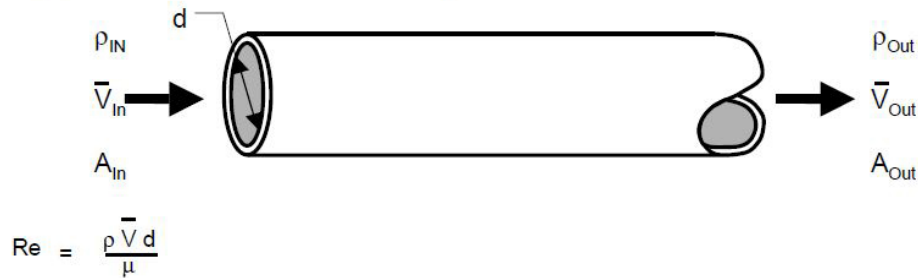


Illustration 2: "Reynolds Number & Pipe Flow" by Smith et al 2002, used under [Creative Commons BY-NC-SA](#) / Cropped from original handout

Where:

μ = dynamic viscosity

ρ = Fluid density

V = fluid velocity

d = Pipe Diameter

						Start	End
Velocity	0.32	meters/second	Reynolds	2108.962	Laminar	0	2100
Velocity	0.605	meters/second	Reynolds	3987.256	Transition	2100	4000
Velocity	0.66	meters/second	Reynolds	4349.734	Turbulent	4000	~

Table 4: Reynolds number calculations.

After figuring out the velocities needed for laminar, transitional, and turbulent flow the static pressure of the fan could be measured to determine if the fan was supplying enough flow to meet the desired demand. As shown in the table below, the average velocity of the fan at low settings was 0.323 meters per second which is right on the edge of

transitional flow. The fan at high speed gave an average velocity of 0.527 meters per second. This is still in the transitional area, although the center velocity for the high fan was in the turbulent range but the flow was not fully turbulent.

Dynamic Pressure						
(Pa)	Center	Midpoint	Edge			
Fan low	0.4	0.6	0.2			
	0.3	0.7	0.3			
	0.3	0.6	0.3			
	0.2	0.6	0.2			
	0.3	0.5	0.2			
	0.4	0.6	0.1			
Avg Fan Low	0.316666667	0.6	0.216667			
Velocity	0.270412373	0.512360286	0.185019	m/s	0.323	
Fan High	0.7	0.6	0.4			
	0.8	0.5	0.5			
	0.9	0.5	0.5			
	0.8	0.4	0.5			
	0.9	0.7	0.3			
	0.9	0.7	0.5			
Average Fan High	0.833333333	0.566666667	0.45			
Velocity High	0.711611508	0.483895826	0.38427	m/s	0.527	

Table 5: Fan pressure calculations.

The other factor for the air velocity is the LI-COR tool has a pump with which is pulls air out of the loop and puts it back in. The LI-COR pump has a flow rate of 1 liter per minute. This results in an air velocity of 0.002 meters per second. This is also an important

fact for the results of the testing. The very low air speed of the LI-COR was used for some of the later testing to simulate natural ventilation.

LI-COR Airflow	1	liter/minute
	0.001	cubic meter/liter
	0.001	cubic meter/minute
	1.66667E-05	cubic meter/second
Area	0.00810321	square meters
	0.002056798	meters/second

Table 6: LI-COR Flowrate.

The mesh membrane could one day be used in ductwork. So, while I had the pressure sensor, I decided to find the pressure drop across the membrane. This was accomplished using the same inlet and outlet openings on the long ends of the PVC loop. The main variable was what was occluding the flow in the blast gate valve. So, several different configurations were tried.

Pressure Test	Pa
No filter cartridge	2.6
With Filter Cartridge	17.3
With Expanded mesh	19.5
with tight mesh	26.2

Table 7: Pressure drop across membranes.

With all the initial testing done, it was time to move to testing the mesh samples for their dehumidification properties. The testing process was to:

1. measure the air outside the PVC loop of the apparatus for a baseline

2. Place sample inlet tube into the apparatus and tape around the inlet to get as good a seal as possible
3. Place the sample in the 3d printed sample holder and insert the holder into the blast gate valve assembly and tape all around the opening for a good seal
4. Turn on the fan to the desired speed (low, high, or off)
5. Measure the CO₂ and H₂O in the apparatus with the LI-COR 7000
6. Using a combination of human breath and water vapor from a room humidifier raise the level of CO₂ up to over 1500 ppm and the H₂O level up to 18-19mmol/mol which was between 56-60% relative humidity.
7. Measure the drop in CO₂ and H₂O over time. When the system seemed to stabilize the power was turned on to the mesh sample using a DC power supply.
8. Continue the measurements for an equal amount of time it took for the mesh to stabilize then turn off the power and remove the sample and start the next test from step 3.

4: Results

The results of the testing were mixed. Since there were several variables, each will be outlined in this section. They include **apparatus leakage, fan speed, mesh size, mesh construction, and electrical input.**

Apparatus Leakage

Due to the small concentrations of water that were being measured it was important to control the air tightness of the testing loop. Despite several methods of sealing used, the loop was never completely airtight. For the remainder of the results, it is important to understand the dynamic mass balance equation (Misztal 2020).

$$C_t = C_{t=0}e^{-\lambda t} + pC_o(1 - e^{-\lambda t})$$

Where:

C_t = Concentration of particle inside the space being studied at time T

$C_{t=0}$ = Concentration of particle inside the space being studied at initial time 0

C_o = Concentration of particle outside the space being studied

λ = Air change rate

T = time

P = penetration factor of particle to space

This equation is assuming that a particle was injected into a space and is not continuing to be deposited and is not being lost to deposition on any of the surfaces but only lost to infiltration. Because the test apparatus is all plastic (PVC, ABS, PLA) it is assumed that it will not absorb H₂O or CO₂. The caulking used to seal the pvc was a waterproof rubber-based material and on top of the already sealed joints was a waterproof tape. So, it is safe to assume that any H₂O or CO₂ loss measured is due to infiltration or to the mesh samples absorption. The CO₂ and H₂O were measured in ppm and mmol/mol respectively every second while logging data. Using the dynamic mass balance equation above another equation was derived to better make sense of both the infiltration and potential mesh water absorption (Misztal, 2020).

$$-\ln \left\{ \frac{C_t - C_0}{C_{t=0} - C_0} \right\} = \lambda t$$

Using this equation and knowing the concentration of H₂O and CO₂ outside of the loop the dynamic air change rate can be computed. This thesis will graph both the air change with time (slope of the line is the air change rate) with which shows the concentration change as well as the air change rate over time which is the integral of the change. It may be easier to think of these two terms as the “velocity” of H₂O or CO₂ loss and the “acceleration” or change in the rate of H₂O or CO₂ loss.

The leakage or infiltration of the loop changed over time as improvements were made, but once final testing commenced no more improvements were made to the system to keep that variable constant. As can be seen in the below leak test the slope of the line which describes the air change rate was 2.7114 air changes per hour. This means that all the air in the loop would be replaced with air from outside the loop 2.7 times per hour. This was unacceptable for being able to capture very small changes in water concentration.

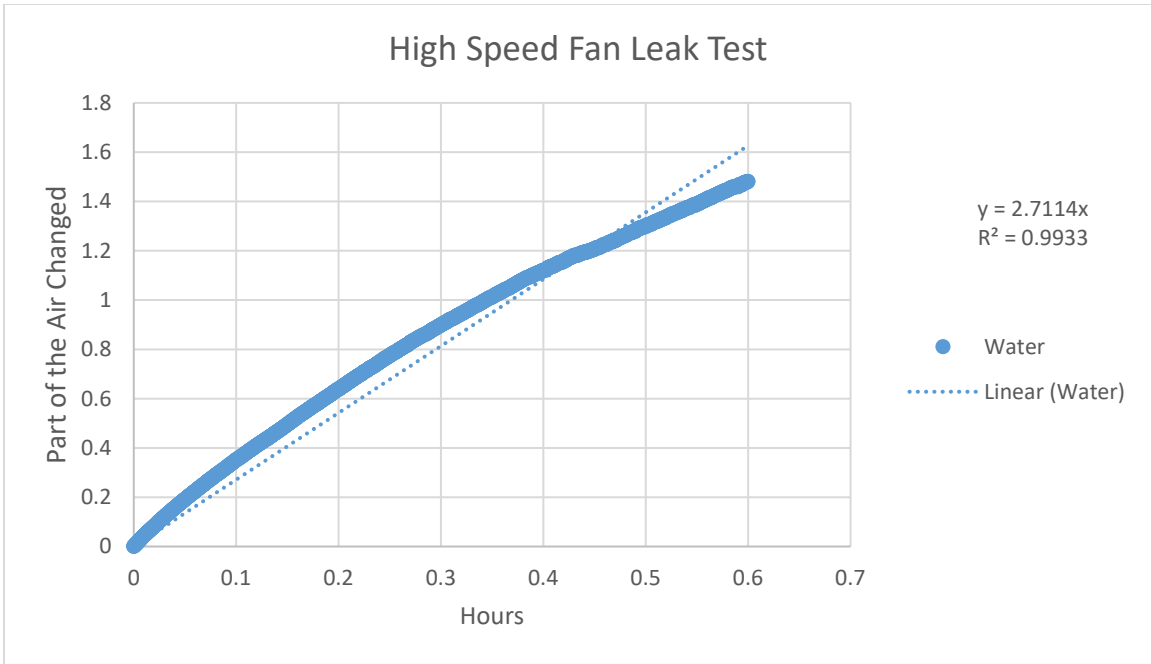


Figure 6: High Speed Fan Leak Test.

After applying significantly more tape and labor, the loop was much better sealed. As shown below the new leakage rate with the fan on high was 0.0755 air changes per hour. This would take around 13 hours for all the air in the system to be replaced by air outside. This was much more acceptable.

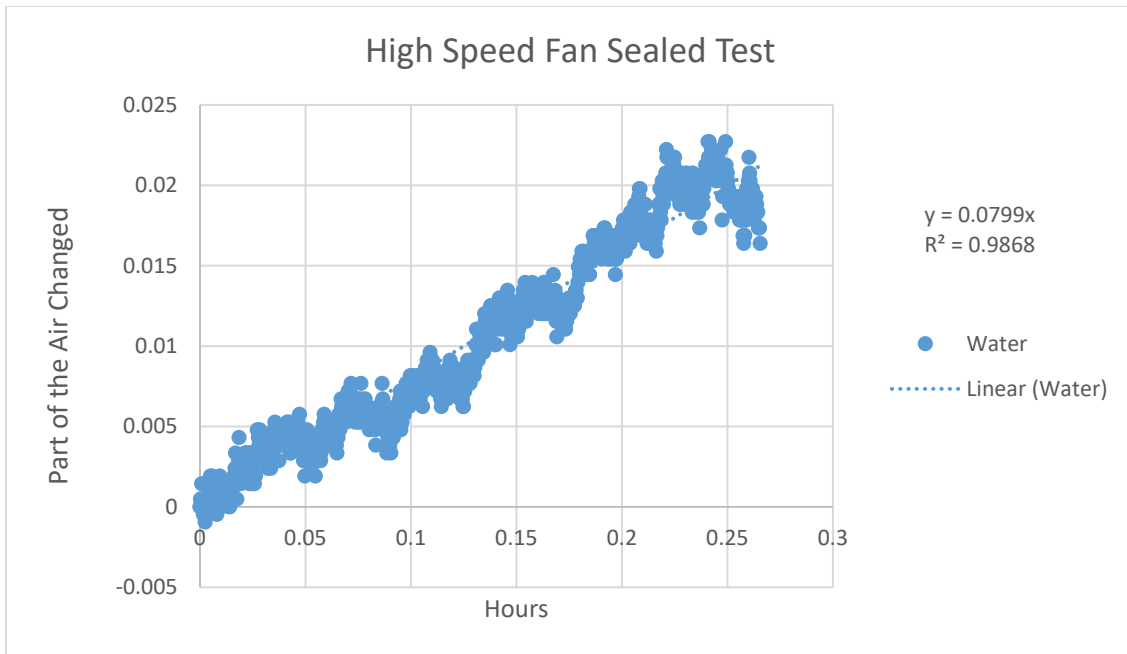


Figure 7: High Speed Fan Sealed Test.

Fan Speed

Throughout the tests it was apparent from the air change rates that the fan was affecting the outcome. The higher the fan speed the bigger the leak got. This makes intuitive sense since the fan is causing a pressure difference between the inside and outside of the loop. It even changed the way the water was absorbed or not absorbed by the mesh samples. As shown in the following graphs the air change rates between H₂O and CO₂ are shown on top of each other.

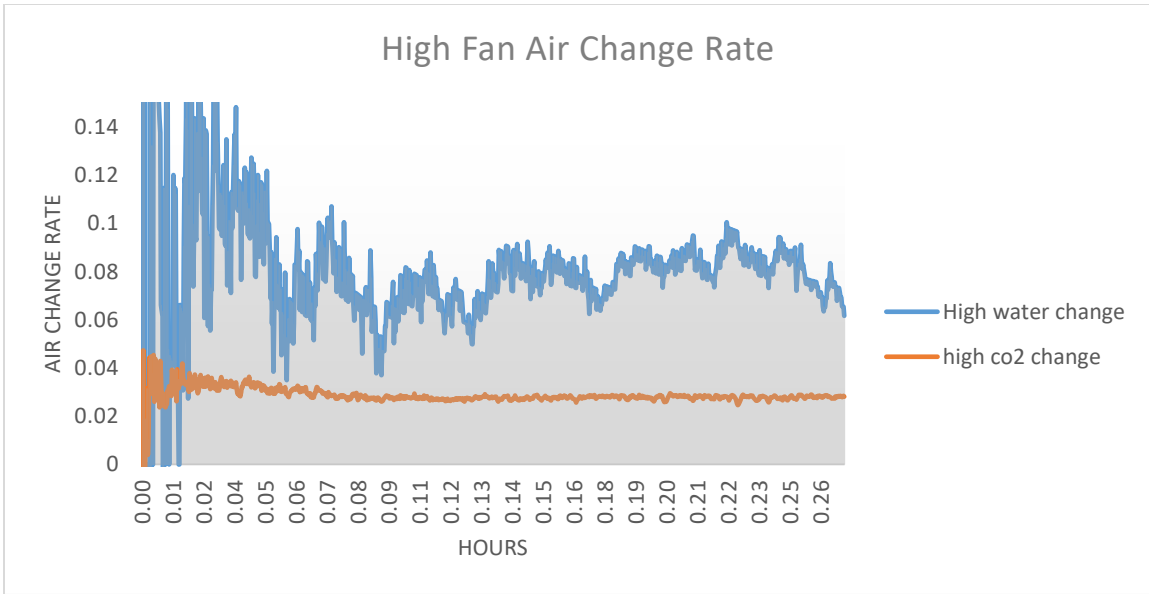


Figure 8: High Fan Air Change Rate.

In the high-speed fan test, the difference in air change rate between H₂O and CO₂ is not very large (0.045 ACH).

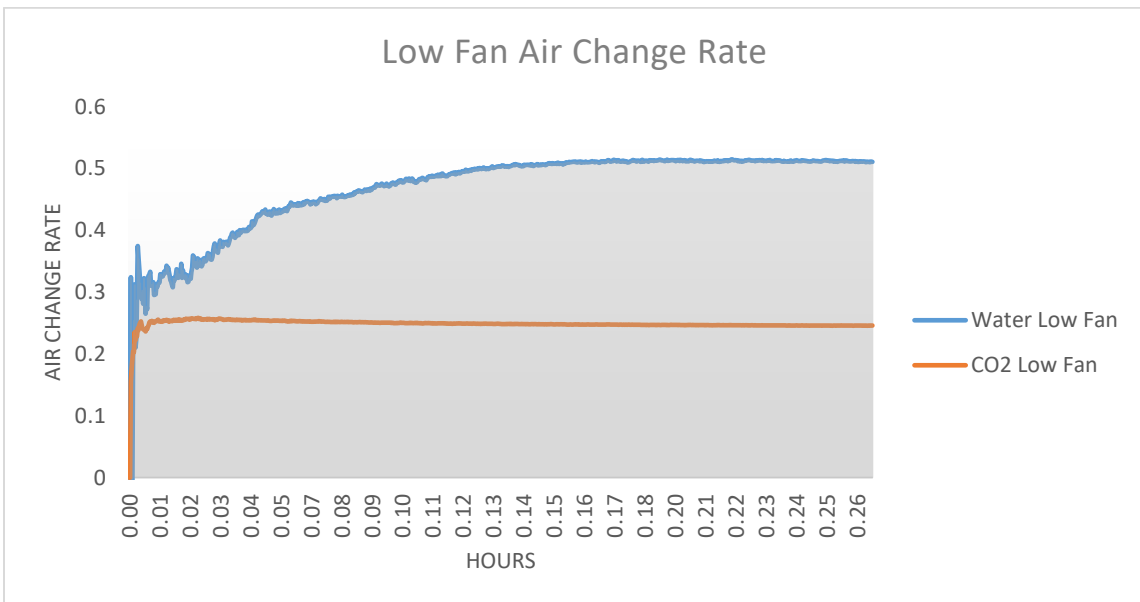


Figure 9: Low Speed Air Change Rate.

In the low fan speed test the difference between the H₂O and the CO₂ was much larger (0.25 ACH).

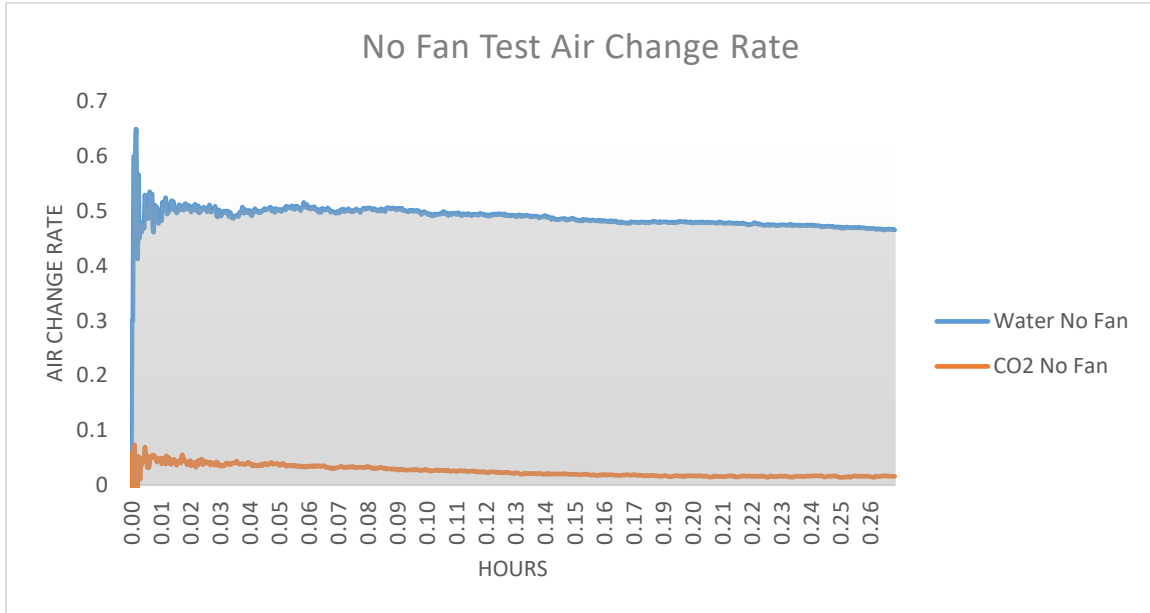


Figure 10: No Fan Test Air Change Rate.

Where the air movement was only supplied by the LI-COR pump (0.002 m/s) the difference between the CO₂ and H₂O air changes was the most dramatic (0.45 ACH).

This will be expanded more in the discussion section, but to get results fast enough to complete the thesis on time, the low fan speed setting was used for all but 2 tests. These two tests were completed to see if the H₂O would come to some sort of equilibrium to determine the H₂O absorption capacity of the samples.

Mesh Size

As mentioned in the methods section there were two different mesh sizes (150/in and 60/in). These two meshes were tested in the same manner but, as was expected, they had different results. The following two graphs show the Mesh A (150/in) and Mesh B(60/in) at the low fan setting. As can be seen the following two graphs (H₂O Mesh A & B), the B Mesh performed better in the same amount of time. The average of the A and B

meshes are pictured in the middle with the best performing mesh and the worst performing mesh bracketing it.

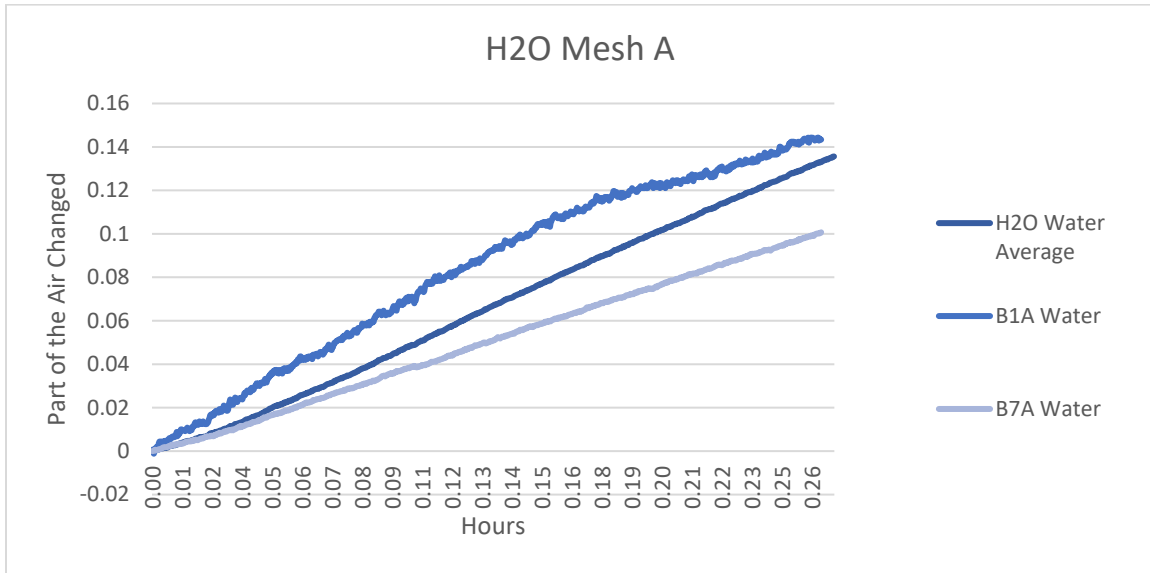


Figure 11: H2O Mesh A.

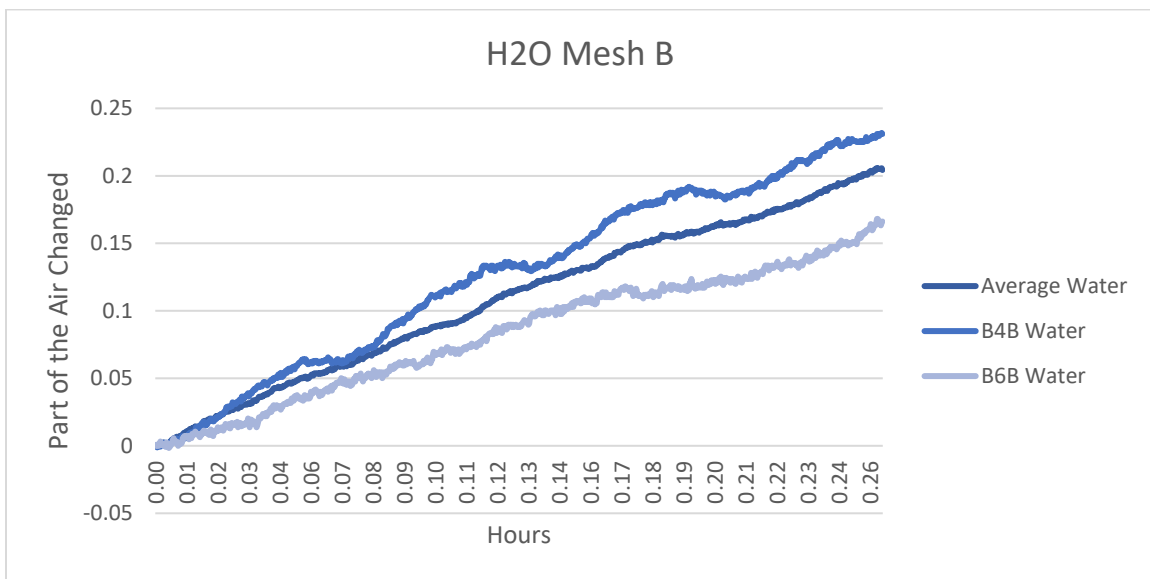


Figure 12: H2O Mesh B.

Mesh Construction

Not only were there 2 different mesh sizes, but there were seven different treatment times applied for each mesh size. The hypothesis was that the researchers who developed the mesh, Kung et al (2018), treated their sample based on its surface area. Nowhere in the literature was a discussion of area to time needed to grow the Copper Oxide 1 & 2 structures. So, the mesh was treated seven different lengths of time in the electrolyte bath shown in figure 13. The following two graphs show the different air change rates for each set of mesh samples.

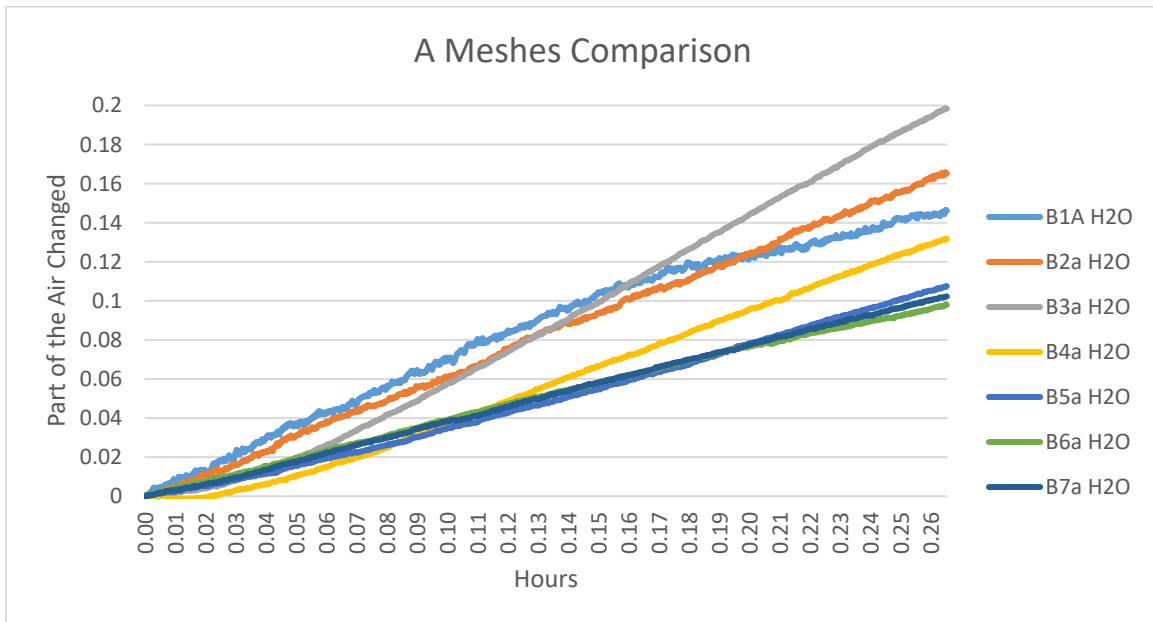


Figure 13: A Meshes Comparison.

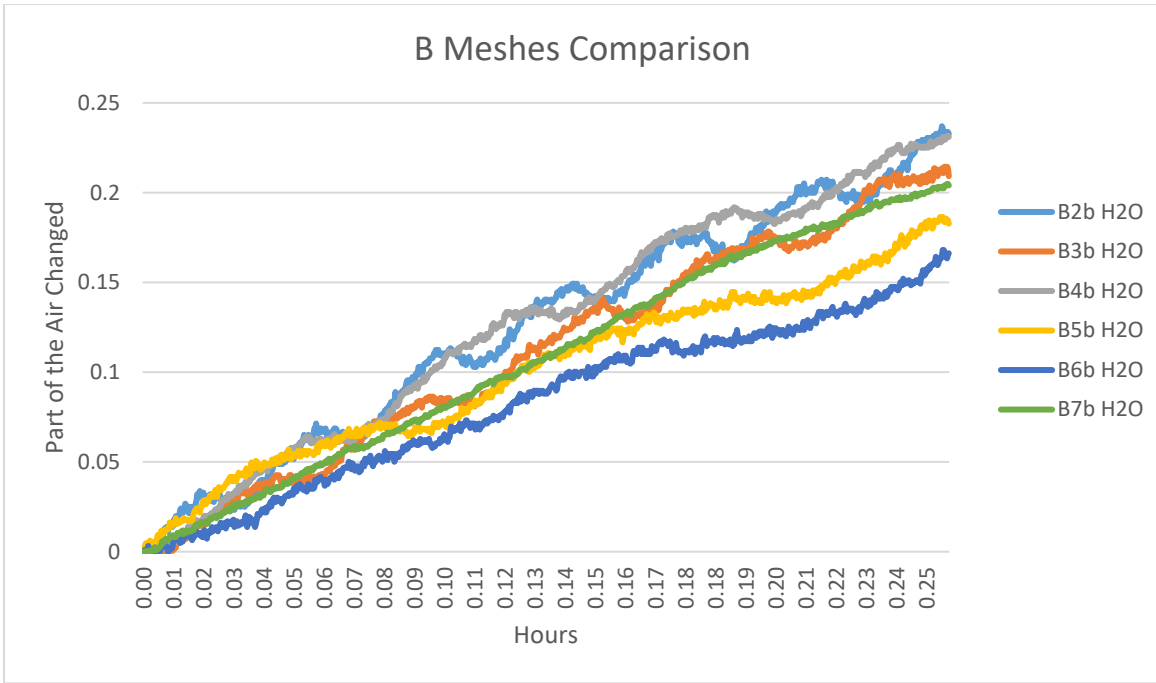


Figure 14: B Meshes Comparison.

Interestingly, for both mesh types, the less coating applied the better. However, when looking at the baseline mesh, the coating is working more than uncoated samples. In the following graph it is apparent that the slopes of the coated A and B meshes are higher than that of the baseline mesh samples with the same pore sizes.

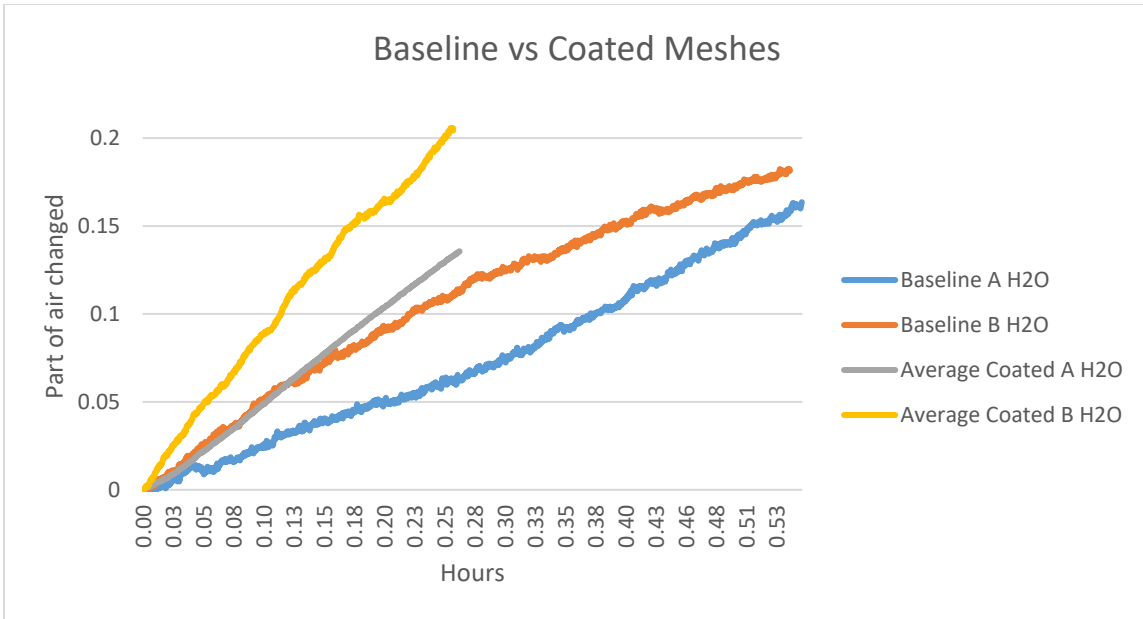


Figure 15: Baseline vs Coated Meshes Comparison.

Electrical Input

Part of the original hypothesis for this trichome mesh was that through specific electrical input the mesh could soak up water and be drained of liquid water by leveraging the meshes superhydrophobic properties. This did not happen as hoped. The electrical input did not seem to have any effect on the mesh’s absorption of water no matter the fan speed, length of time, or mesh. The following two graphs show two different meshes that were run for longer periods of time than usual to discover if the electrical properties of the mesh can be determined when the rate of change has stabilized.

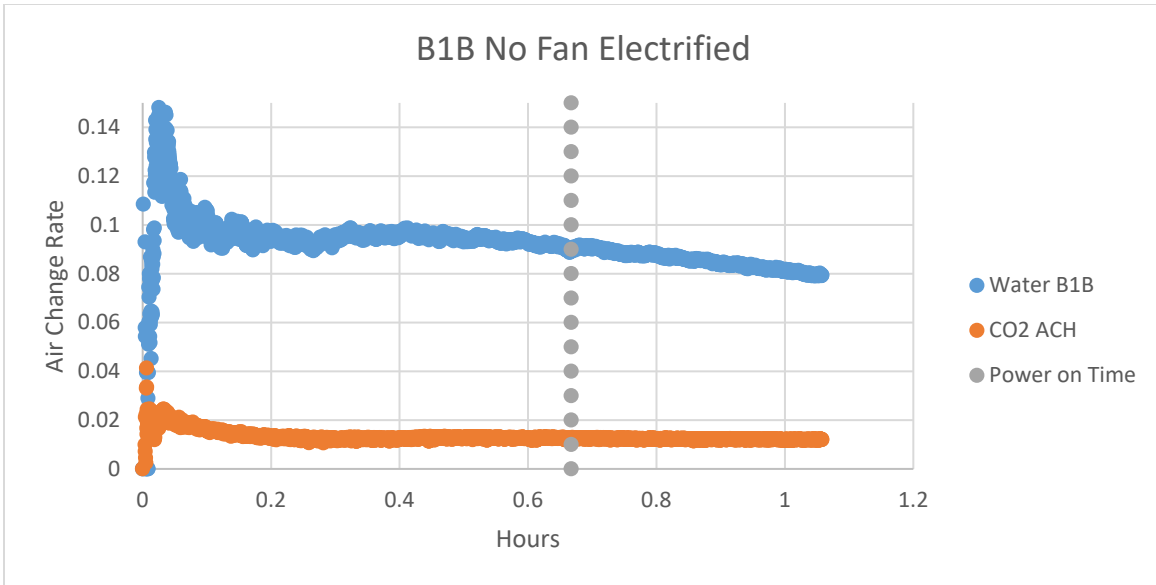


Figure 16: B1B No Fan Electrified Air Change Rate.

This test ran for a whole hour, and the last 25 minutes or so the mesh had electrical current running through it. The air change rate was already going down slightly when the power was turned on, but no appreciable change in slope was noticed upon turning on the power.

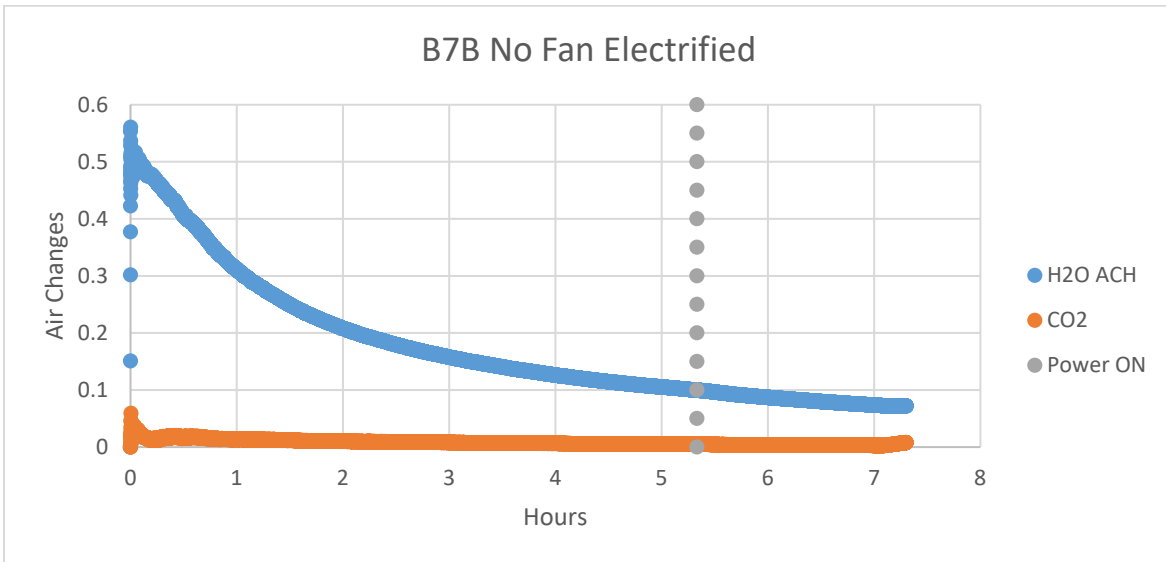


Figure 17: B7B No Fan Electrified.

This test was an extreme one done at the very end of the thesis study. It was run for the whole workday with 5 hours for the mesh to stabilize and another 2 for the electrification to display some change. Unfortunately, there was no appreciable change detected. However, this test did provide some more useful information.

Passive Water Absorption

The last test attempted was a workday long (8 hours) between preparing the mesh, the equipment, and taking measurements. This test was completed without the internal fan to give the system as much of a chance to seal as possible. The tape was checked and rechecked to seal any openings that may have been missed. The results in air change were shown in the table above (B7B No Fan Electrified). The CO₂ and Water concentration results over time are shown below.

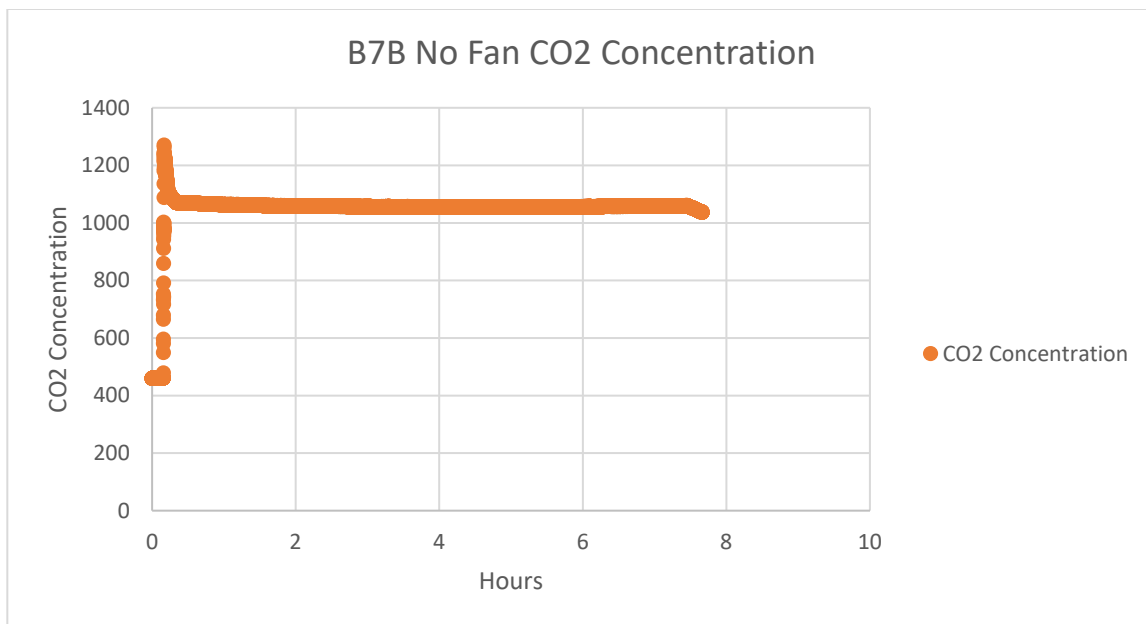


Figure 18: B7B No Fan CO₂ Concentration.

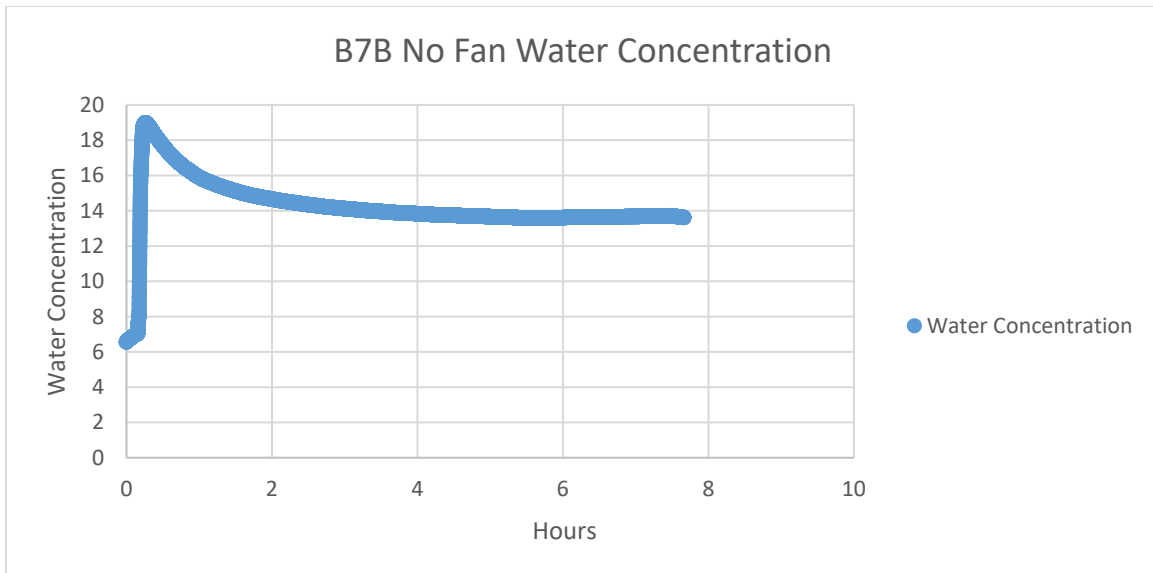


Figure 19: B7B No Fan Water Concentration.

The loss rate of CO₂ is extremely low (0.0062 ACH or around 161 hours/6.7 days to fully change the air) while the loss rate of water vapor is modest (starting at 0.5ACH and ending the test at around .07ACH). Looking at the concentration graphs the CO₂ stabilizes very quickly fixed concentration while the water concentration continues to drop from 19 mmol/mol down to just below 14mmol/mol.

5: Discussion and Conclusion

The results of the test are mixed. It seems like there are several takeaways to be discussed.

1. The fan speed makes a difference in water absorption.
2. The mesh size and construction make a difference in absorption.
3. The electrical input does not seem to make a difference for adsorption or desorption.
4. The mesh does seem to passively absorb water.

Fan Speed

The air speed moving through the loop and sample seems to influence absorption. This could be for several reasons. The first is that the increase in air velocity creates a pressure difference between inside and outside of the testing apparatus which permits the large concentrations of CO₂ and H₂O in the apparatus to be diluted by the lower concentration air outside the loop. The second reason is that way the LI-COR 7000 measures H₂O is different than the way it measures CO₂, and the higher fan speed is better mixing the air. The third reason is that the mesh is passively absorbing water, and the higher fan speed is actively drying the mesh or causing the air to reabsorb the water weakly bonded to the mesh. A test should be designed to determine which of the three or combination of the three are correct.

Mesh size and Construction

One of the discoveries of the study was that there is a discernable difference between the two mesh sizes and the times that the mesh was treated in the electrolyte solution. The most counterintuitive thing discovered is that the B type meshes which have more open area per inch than the tight knit A type mesh performed best. Also counterintuitive was that there was an optimal amount of coating for the mesh type B3A outperformed the other mesh samples in the A group while B4B outperformed the other samples in the B group. This could be used to infer that there is a sweet spot between being coated and non-coated for the passive absorption of water. More testing and measurements are needed to determine where this sweet spot lies and how it can be quantified.

Electrical input

The hypothesis that the electrical properties of this mesh dehumidification membrane could help it to drain liquid water seems to be wrong. The most probable reason for this is the original mesh sample (Kung et al, 2018) was used to separate liquid water from liquid oil. The liquid state of the water allowed the mesh to leverage the surface tension properties of water, but in the same study the researchers found that after switching

to its superhydrophilic state the mesh would have to be air dried before it was superhydrophobic again. Because dehumidification deals with vapor water instead of liquid, there is no surface tension force to make the water bead up on the artificial trichomes of the mesh. Water vapor bypassed the trichome tips and was absorbed passively by the copper oxide 1 crystals. The original mesh by Kung et al worked by turning the tips of the crystalline mesh that were copper oxide 2 (which does not bond with water) into copper oxide 1 by adding electricity. This affect is bypassed by interacting with vapor rather than fluid. This could also shed light on why the less coated mesh samples were better able to absorb water, because there was less copper oxide 2 coating on them.

Passive Water Absorption

If the assumption that the LI-COR measures H₂O and CO₂ at the same rate is correct, then it would seem the mesh samples do passively absorb water. The best example of this is the last test completed (B7B No Fan). While the CO₂ quickly came to equilibrium, the H₂O took a long time to come to equilibrium and even then, was not yet at the same loss rate as the CO₂. This suggests that the mesh was indeed absorbing water vapor. The water vapor levels in the test went from 18.889mmol/mol down to 13.607mmol/mol which is a change of 5.382 mmol/mol. Using some quick conversions, we see that:

5.382	mmol/mol change with mesh
6.607422905	mmol water removed
18	g/mole water
0.018	g/mmole water
0.118933612	g water removed by screen
3.459857143	change in absolute humidity g/kg
0.003459857	absolute humidity change kg/kg

Table 8: Mesh Water Absorption calculations.

Our mesh absorbed 0.1189 grams of water. This might not seem like a lot but for the volume of the pvc loop that is a change in humidity of 0.00345 kg water/kg air. Earlier it was mentioned that the 19mmol/mol starting point at the room temperature of 25 that the apparatus was measured to be 60% relative humidity. Using a psychrometric chart from ASHRAE we see that the change in enthalpy using this mesh is 8.6 kJ/kg of dry air. This occurred over the course of 435 minutes or 26,100 seconds. If the flow rate of the LI-COR pump is taken into consideration (0.002 m/s) then the membrane soaked up that 8.6 kJ/kg from 0.435 cubic meters of air (looped flow for a given time) which would give us 74kj. Since this occurred over the 26,100 seconds this occurred at a rate of 0.14 Watts.

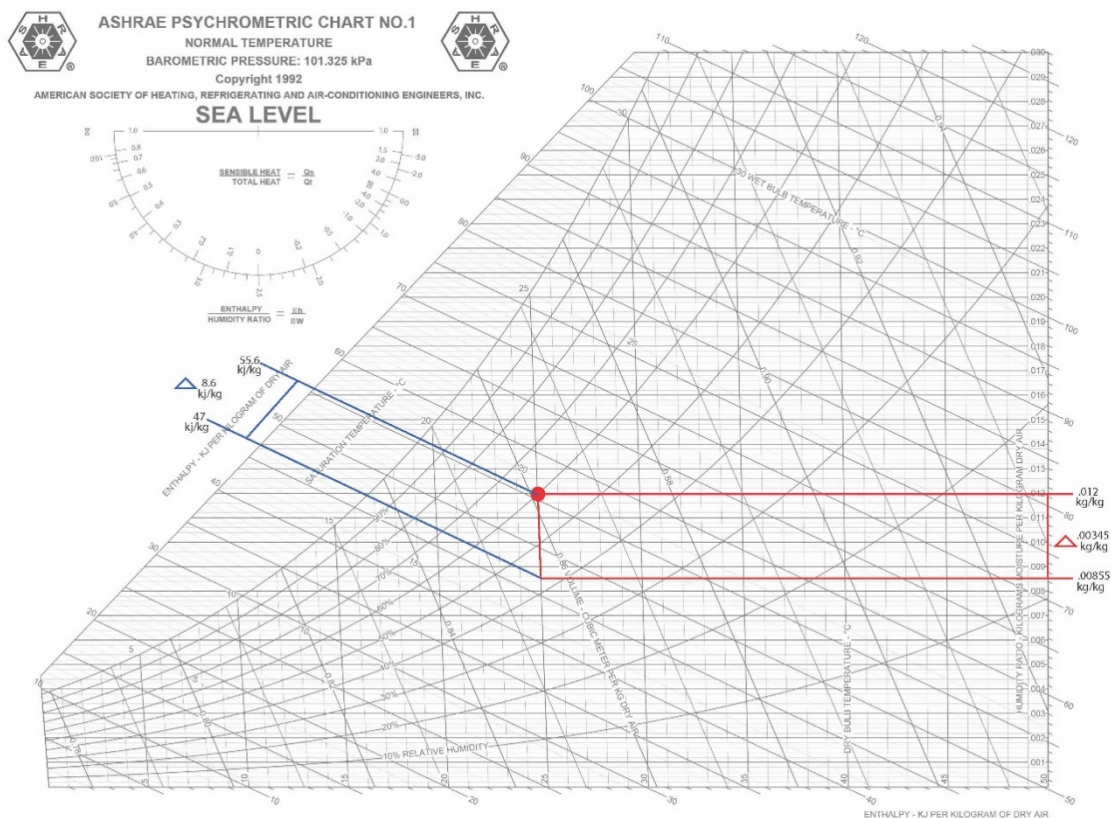


Illustration 3: Dehumidification by mesh illustration, ASHRAE 1992.

Apparatus Sizing

A note on the sizing of the testing apparatus is required before the concluding remarks. The testing apparatus was sized in order not to have problems in two different scales. The first potential problem was the accuracy of the LI-COR device. If the error rate of the LI-COR was ± 0.1 mmol/mol of water vapor but the loop only allowed 1 mmol/mol of water vapor to be present in order to reach the $\sim 60\%$ relative humidity mark the error rate of the test would be 10% which is not acceptable. So the amount of air in the loop needed to be big enough that the ± 0.1 mmol/mol of water vapor measured by the LI-COR would be a small error overall. The second potential problem was the scale of test being too large for differences in humidity to be detectable. In the research facility where the tests were completed there are room sized chambers where humidity and temperature can be controlled. However, if the small 4 inch diameter mesh sample only took out 0.1189 grams of water in a room sized chamber with orders of magnitude more water vapor, the change in overall relative humidity would be too small to be measured. This is why the pvc loop was sized so that the \pm error rate of the LI-COR was 1% but no larger.

Conclusion

In conclusion, this thesis aimed to answer this research question: Is there a way to dehumidify air electrochemically or mechanically like biological systems (lotus leaf, air plants) rather than using psychometrics, which are energy intensive, or desiccants, which require drying and eventual replacement?

The literature review indicated that it may be possible with the mesh developed by Kung et al (2018). The resulting hypothesis was that the copper mesh when treated would dehumidify the air using the superhydrophobic and superhydrophilic properties it was imbued with from an electrolysis process. Converting liquid water from the water vapor to drain away as a possible sustainable method of dehumidification.

In the methodology, it was outlined how the mesh was created following as closely as possible to the method described by Kung et al.

In the results and discussion, the experiment tests indicated that the fan speed, mesh type, and mesh construction influenced the water absorption rate while the electrical input did not. Doing some back of the napkin math, it was determined that the B7B mesh absorbed water at a rate of 0.11 Watts but seemed to have almost reached its capacity by the end of the 7-hour test.

The results of the thesis do not prove the initial hypothesis that the mesh can be made to form liquid water to be drained away. The study did determine that the copper oxide coating passively dehumidified the air. It is possible that with more mesh surface area, a more discernable electrical response may be measured, but more testing is required.

Future research into this material could compare it to existing desiccant systems for passive dehumidification potential and the energy needed to desorb water for each system. Future research into the electrical responses of the Kung et al mesh could increase the surface area of the mesh to determine if the electrical response is present for large surface area meshes. Similar studies could look into the response to electrical input without air movement and in an environment where desorption will not occur without energy input like a 100 percent relative humidity environment.

References

- American Society of Heating, Refrigerating and Air-Conditioning Engineers.
2007. *Ventilation for acceptable indoor air quality: ASHRAE standard*. Atlanta, GA:
American Society of Heating, Refrigerating and Air-Conditioning Engineers.
- American Society of Heating, Refrigerating and Air-Conditioning Engineers. 2017. *Thermal
Environmental Standards for Human Occupancy: ASHRAE standard*. Atlanta, GA:
American Society of Heating, Refrigerating and Air-Conditioning Engineers.
- American Society of Heating, Refrigerating and Air-Conditioning Engineers.
1992. *Psychrometric Chart NO. 1, Normal Temperature, Barometric Pressure 101.325
KPa*. Atlanta, GA: American Society of Heating, Refrigerating and Air-Conditioning
Engineers.
- Benyus, Janine M. *Biomimicry Innovation Inspired by Nature*. New York: Harper Perennial,
1997.
- Bornehag, C.-G., G. Blomquist, F. Gyntelberg, B. Jarvholm, P. Malmberg, L. Nordvall, A.
Nielsen, G. Pershagen, and J. Sundell. “Dampness in Buildings and Health. Nordic
Interdisciplinary Review of the Scientific Evidence on Associations between Exposure to
‘Dampness’ in Buildings and Health Effects (NORDDAMP).” *Indoor Air* 11, no. 2 (May
31, 2001): 72–86. <https://doi.org/10.1034/j.1600-0668.2001.110202.x>.
- Cheng, Yang-Tse, and Daniel E Rodak. “Is the Lotus Leaf Superhydrophobic?” *Applied
Physics Letters* 144101, no. 86 (March 30, 2005).
<https://doi.org/https://doi.org/10.1063/1.1895487>.

Ensikat, Hans J, Petra Ditsche-Kuru, Christoph Neinhuis, and Wilhelm Barthlott.

“Superhydrophobicity in Perfection: the Outstanding Properties of the Lotus Leaf.” *Beilstein Journal of Nanotechnology* 2 (October 2011): 152–61.

<https://doi.org/10.3762/bjnano.2.19>.

Harriman, Lewis G. *The Dehumidification Handbook*. Amesbury, MA: Munters Corporation, 1989 and 2002.

Harriman, Lewis G. "Dehumidification equipment advances." *ASHRAE journal* 44.8 (2002): 22.

Kim, Moon Keun, and Hansjürg Leibundgut. “Advanced Airbox Cooling and Dehumidification System Connected with a Chilled Ceiling Panel in Series Adapted to Hot and Humid Climates.” *Energy and Buildings* 85 (September 28, 2014): 72–78.
<https://doi.org/10.1016/j.enbuild.2014.09.031>.

Kim, Moon Keun, and Hansjürg Leibundgut. “A Case Study on Feasible Performance of a System Combining an Airbox Convectector with a Radiant Panel for Tropical Climates.” *Building and Environment* 82 (October 19, 2014): 687–92.
<https://doi.org/10.1016/j.buildenv.2014.10.012>.

Kung, Chun Haow, Beniamin Zahiri, Pradeep Kumar Sow, and Walter Mérida. “On-Demand Oil-Water Separation via Low-Voltage Wettability Switching of Core-Shell Structures on Copper Substrates.” *Applied Surface Science* 444 (February 28, 2018): 15–27.
<https://doi.org/10.1016/j.apsusc.2018.02.238>.

La, Duc-Duong, Tuan Anh Nguyen, Sungho Lee, Jeong Won Kim, and Yong Shin Kim. “A Stable Superhydrophobic and Superoleophilic Cu Mesh Based on Copper Hydroxide

Nanoneedle Arrays.” *Applied Surface Science* 257, no. 13 (January 25, 2011): 5705–10.
<https://doi.org/10.1016/j.apsusc.2011.01.078>.

Lusa, Makeli Garibotti, Elaine Cristina Cardoso, Silvia Rodrigues Machado, and Beatriz Appezzato-Da-Glória. “Trichomes Related to an Unusual Method of Water Retention and Protection of the Stem Apex in an Arid Zone Perennial Species.” *AoB PLANTS* 7 (January 2015). <https://doi.org/10.1093/aobpla/plu088>.

Misztal, Pawel. "Mass Balance Dynamic Solution and Special Case." *Indoor Air Quality*, Spring 2020, The University of Texas at Austin, Austin, TX. *Class notes*.

Oh, Seung Jin, Kim Choon Ng, Wongee Chun, and Kian Jon Ernest Chua. “Evaluation of a Dehumidifier with Adsorbent Coated Heat Exchangers for Tropical Climate Operations.” *Energy* 137 (March 9, 2017): 441–48.
<https://doi.org/10.1016/j.energy.2017.02.169>.

Pan, Qinmin, Min Wang, and Hongbo Wang. “Separating Small Amount of Water and Hydrophobic Solvents by Novel Superhydrophobic Copper Meshes.” *Applied Surface Science* 254, no. 18 (March 15, 2008): 6002–6.
<https://doi.org/10.1016/j.apsusc.2008.03.034>.

Smith Joseph Jr., and Culpepper Martin. ”*Reynolds Number and Pipe Flow, study materials*” 2.000 *How and Why Machines Work*. Spring 2002. Massachusetts Institute of Technology: MIT OpenCourseWare, <https://ocw.mit.edu>. License: [Creative Commons BY-NC-SA](https://creativecommons.org/licenses/by-nc-sa/4.0/). <https://ocw.mit.edu/courses/mechanical-engineering/2-000-how-and-why-machines-work-spring-2002/study-materials/TurbulentFlow.pdf> accessed: 4/28/21

- Sun, Manhui, Chunxiong Luo, Luping Xu, Hang Ji, Qi Ouyang, Dapeng Yu, and Yong Chen. “Artificial Lotus Leaf by Nanocasting.” *Langmuir* 21, no. 19 (July 22, 2005): 8978–81. <https://doi.org/10.1021/la050316q>.
- Yanlong, Shi, Yang Wu, Feng Xiaojuan, Wang Yongsheng, Yue Guoren, and Jin Shuping. “Fabrication of Superhydrophobic-Superoleophilic Copper Mesh via Thermal Oxidation and Its Application in Oil–Water Separation.” *Applied Surface Science* 367 (January 28, 2016): 493–99. <https://doi.org/10.1016/j.apsusc.2016.01.233>.
- Yin, Wei, Guoqiang Zhang, Wei Yang, and Xiao Wang. “Natural Ventilation Potential Model Considering Solution Multiplicity, Window Opening Percentage, Air Velocity and Humidity in China.” *Building and Environment* 45, no. 2 (June 15, 2009): 338–44. <https://doi.org/10.1016/j.buildenv.2009.06.012>.
- Zhang, Yufan, and Peter Barrett. “Factors Influencing the Occupants’ Window Opening Behaviour in a Naturally Ventilated Office Building.” *Building and Environment* 50 (October 15, 2011): 125–34. <https://doi.org/10.1016/j.buildenv.2011.10.018>.